A MICROFABRICATED NEURAL PROBE WITH POROUS SI-PARYLENE HYBRID STRUCTURE TO ENABLE A RELIABLE BRAIN-MACHINE INTERFACE

Tao Sun[1], Srinivas Merugu[1], Wei Mong Tsang[1, 2], Woo-Tae Park[1,3], Ning Xue[1], Yunxiao Liu, Beibei Han[1], Gavin Dawe[4] and Alex Yuandong Gu[1*]*

[1]Institute of Microelectronics, Agency for Science, Technology and Research (A*STAR), SINGAPORE

[2]The Hong Kong Applied Science and Technology Research Institute (ASTRI), Hong Kong, CHINA

[3]Department of Mechanical and Automotive Engineering, Seoul National University of Science and Technology, Seoul, KOREA

[4]Department of Pharmacology, National University of Singapore, SINGAPORE

ABSTRACT

To establish a reliable brain-machine interface (BMI), we report for the first time, a multifunctional porous silicon (PSi)-parylene neural probe using a CMOS compatible fabrication process. The biodegradable PSi shank serves as a mechanical stiffener for insertion process, then dissolves to leave only the polymeric structure to reduce stiffness mismatch between implant and cortical tissue, thus attenuates tissue responses. Moreover, its porous structure can serve as drug reservoir. The healing of the insertion trauma can be enhanced by continuously releasing pre-loaded drugs with the PSi degradation. Hence, the neural probe enables a more reliable BMI.

INTRODUCTION

Invasive Brain-machineinterface (BMI) technologies focus on restoring the lost body functions such as control, sensory and motor capabilities, for patients via stimulating neural tissues and/or recording extracelluar potentials from surrounding neurons. However, the lifetime of the introcortical probes recording neural signals has been reported to last for several years or even a few weeks, and cannot meet requirements of clinical applications [1]. The recording interrupted by the loss of signal is most likely due to both acute and chronic host tissue responses. The acute inflammation in cortical tissues is initiated by the mechanical trauma of probe insertion, finally resulting in the formation of thick nonconductive fibrous tissue surrounding the probes [2]. Due to the relative micromotion and mechanical mismatch between delicate cortical tissues (~100KPa) and rigid neural probe (~190GPa, Si), post implantation injury or local tissue damage keeps occurring to deteriorate the chronic host tissue responses and long-term signal recording stability. Therefore, many scientific and technological efforts are devoted to reducing host tissue responses and establishing stable BMI by means of designing various neural probe geometry, employing more biocompatible and flexible materials, incorporating drug delivery system into neural probes, etc [3-5]. But there are still no definitive solutions for the long-term reliable BMI.

Compared to other approaches to reduce the host tissue responses, the neural probe with adaptive stiffness is attracting ever-growing attention, since it has not only enough mechanical strength to penetrate through the cortex, but can also significantly reduce the Young's modulus to become closer to the cortical tissue modulus. Various biodegradable coatings (e.g. silk [6]) were proposed to temporally strengthen polymeric probe prior to the insertion. As these coating materials are much softer than Si, thick coating layers (> 500 μm) are required to facilitate the insertion process, resulting in an excessive surgical trauma. With its biocompatibility, mechanical properties and biodegradability, porous silicon (PSi) is a promising candidate as a temporary mechanical stiffener for polymeric probes. However, there are technical challenges to integrate the fabrication of PSi shank with polymeric structures.

In this study, we propose a novel CMOS compatible microfabrication process to develop a PSi-parylene neural probe. Additionally, mechanical properties, drug-loading capability, biodegradability and *in vivo* host tissue responses to PSi shanks were investigated.

DESIGN

The PSi-parylene neural probe consists of PSi shanks and polymeric structure made of two layers of parylene-C with a Ti/Au in-between metallization. The mechanical strength and degradation rate of PSi shank can be tailored by its porosity. The PSi shank is stiff enough to penetrate into cortical tissue, and then gradually degrades in brain. Eventually, the remaining thin parylene-C insulting layers (~5μm) maintain flexibility to attenuate the post-implantation injury. Moreover, the acute host tissue responses can be reduced by continuously releasing anti-inflammation drugs/biomoleculars with the PSi degradation, as drugs can be loaded into the porous structure of PSi. Therefore, BMI reliability is expected to improve. In this study, PSi shanks with 70% porosity were developed.

Microfabrication process

8-inch Si wafers (p-type, (100) oriented, 0.002~0.005 ohm-cm) used in this study were purchased from Sumco (Sumco Corp. Japan). The CMOS compatible microfabrication process is illustrated in Fig. 1. Briefly, 0.3 μm thick SiN_x layers were deposited on both sides of the Si wafer via low pressure chemical vapor deposition (LPCVD) technology as the hard mask to trench and porosify Si in an anodization process (Fig. 1a). After patterning frontside SiN_x layer, a deep reactive ion etching (DRIE) process was

carried out to form deep trenches (70 µm) into the Si substrate to define the thickness and profile of PSi shanks (Fig. 1b). For porosification (done via anozidation), it was essential to create a conductive path through the wafer thickness. Hence the backside LPCVD SiN_x layer was removed using RIE. Selective porosification of silicon through the frontside LPCVD mask was carried out by anodizing the silicon wafer in a 1:1 (v/v) mixture of aqueous hydrofluoric acid (49% HF) and ethanol (99.5%), for 35 min. (Fig.1c).Subsequently, the frontside SiN_x mask was removed, followed by annealing the porosified wafers in oxygen environment at 600 °C for 10 min to stabilize the surface properties of PSi. 300 nm-thick SiO_2 thin film was then deposited via plasma enhanced chemical vapor deposition (PECVD) to prevent contamination from parylene fabrication (Fig. 1d). Afterwards, two parylene-C insulating layers (~5µm) and Ti/Au in-between metallization were fabricated on PSi shanks (Fig. 1e-h). The fabrication of the sandwich structure was similar to that of report [7]. To protect the parylene-C structure during subsequent backside grinding process, a layer of photoresist (PR) was coated on the top, and the wafer was then bonded to a handle wafer via a layer of double-side thermal tape (Fig. 1i). A back-side grinding process was performed to attenuate the thickness of the patterned wafer to 50 µm (Fig. 1j). Finally, the PSi-parylene probes were released by dicing the wafer and soaking chips in acetone, IPA and ethanol solution separately (Fig. 1k).

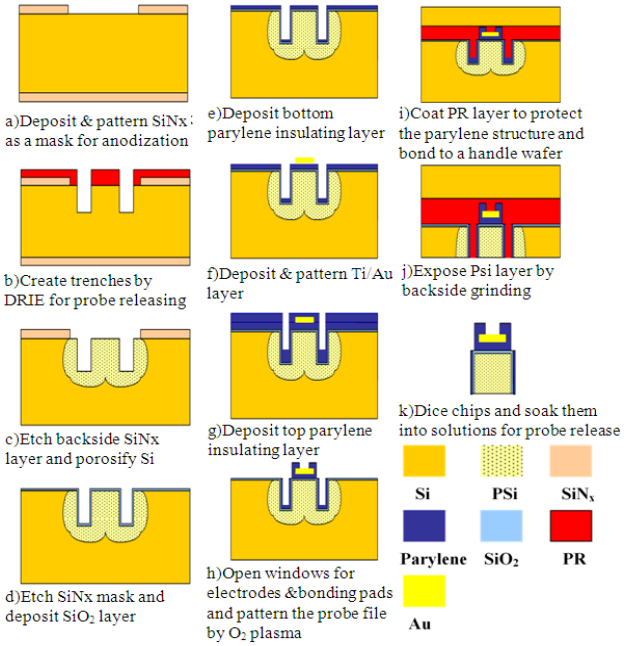

Figure 1: CMOS compatible microfabrication process of the PSi-parylene neural probe.

Methods

Scanning electron microscopy (SEM) was used to characterize the surface morphology and cross-section morphology of samples. The buckling force of the PSi shank was simulated by finite element software (COMSOL Multiphysics 5.0). To demonstrate the drug-loading capability of the PSi shank, 1 mg/ml Dex fluorescein solution in artificial cerebrospinal fluid (ACSF) was used to soak Si and PSi shanks at room temperature for half an hour. After being rinsed by ACSF and distilled water (DIW), and dried in adesiccators, the soaked Si and PSi shanks were observed using a fluorescence microscope. Biodegradability of PSi shank was evaluated by an ammonium molybdate colorimetric assay [8]. The principle of the assay is to evaluate silicic acid produced during the degradation of PSi shanks. In aqueous solutions, the native SiH_x functional groups on PSi surface and bulk Si with nano-featured porous structure are prone to be oxidized into soluble SiO_2 (Eqs. (1) and (2)), and the final degradation products consist of various silicic acid compounds with the orthosilicate (SiO_4^{4-}) ion as the basic building block (equation (3)) [9].

$$SiH_x + H_2O \rightarrow SiO_2 + 4H_2 \quad (1)$$

$$Si + O_2 \rightarrow SiO_2 \quad (2)$$

$$SiO_2 + 2H_2O \rightarrow Si(OH)_4 \quad (3)$$

To verify that the PSi shank is stiff enough to penetrate into brain tissues, *in vivo* insertion tests were carried out, and all surgical procedures were approved by the Institutional Animal Care and Use Committee of National University of Singapore. Rectangular holes (5 × 0.6 mm) above cortex were drilled 1 mm posterior to bregma, 1 mm anterior to lambda, 2 or 4 mm lateral to the midline. Dura mater was then incised and deflected. Eventually, Si and PSi shanks were implanted stereotaxically and lowered slowly into the neocortex. Immunohistochemical staining was carried out for insertion sites to quantitatively compare the tissue responses. After 10 weeks of implantation, adult Male Sprague Dawley rats (250 ~ 300 g, n=5) were prepared for immunohistochemistry, using methods similar to those previously described [1].

RESULTS AND DISCUSSION

Fig. 2a shows the surface morphology of PSi after the anodization process. Irregular and nano featured pores (11.1±7.6 nm) were visualized and uniformly distributed across the surface. The cross-section morphology of PECVD SiO_2 protective layer on PSi is displayed in Fig. 2b. The SiO_2 layer has intimate contact with PSi substrate, and no crack or delamination was present, indicating that the SiO_2 can effectively protect the porous structure from parylene deposition, and serve as the substrate for the formation of the polymer structure. Moreover, obvious branching of the pores is visible and the pores are interconnected. Due to a preferential pore propagation along the (100) crystallographic direction, the porous structure vertically formed on the Si substrate. The scratches generated by the backside grinding process are present on the backside of the PSi shank and no cracks occur along the PSi shank (Fig. 2c), revealing that the porous structure can sustain the mechanical grinding process. Hence, the PSi shank can be successfully released after the backside grinding and soaking processes.

The optical images of the PSi-parylene neural probe are shown in Fig. 3. The neural probe with a comb-like structure has 5 PSi shanks (4 mm in length, 150 µm in

width, and 55 µm in thickness), and there are 4 gold recording sites (ø30 µm) on each shank (Fig. 3a). Accordingly, 20 gold bonding pads are designed on the backend for electrical connection (Fig. 3b). To assist in penetration through cortex and minimize the damage zone during insertion, the PSi shank has a sharp corner with an angle of 17°, while the parylene insulating layers had a round shape at the tip to reduce inflammations or local tissue damages after PSi dissolved.

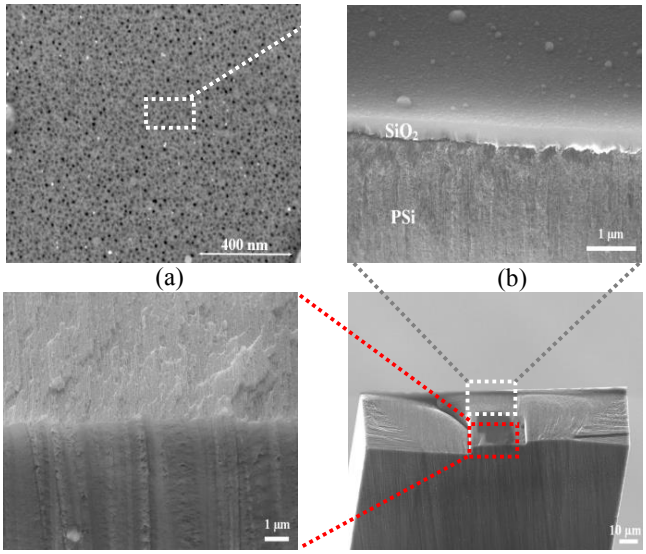

Figure 2: SEM of (a) *surface morphology of PSi; (b) cross sectional morphology of PSi and SiO_2 protective layer; (c) cross sectional morphology of PSi after backside grinding; (d) cross sectional morphology of a PSi shank.*

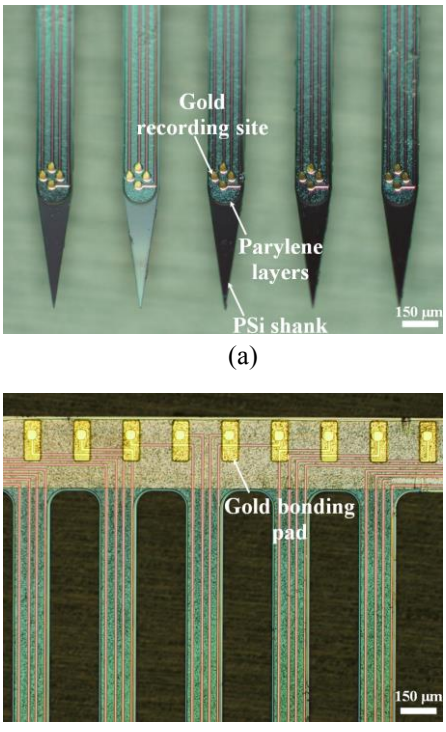

Figure 3: (a) *Tips of PSi shanks with parylene insulating layers and gold recording sites; (b) bonding pads on the backend of the PSi-parylene probe.*

The mechanical strength of the PSi shank was estimated from the critical buckling load formula (Euler buckling formula). When the applied force during insertion is larger than F_{cr}, the PSi shank deforms into a buckled configuration which is adjacent to the original configuration. According to the geometry of the PSi shank, its critical buckling force was predicted to be 26.2 mN (Fig. 4a). Depending on probe size, probe geometry, insertion rate, insertion location, the maximum insertion force required for implantation into rat cortex was reported to be less than 3 mN [10], indicating that the PSi shank can offer mechanical reliability and safety during implantation. Fig. 4b shows the insertion of Si and PSi shanks into a rat brain. Both Si and PSi shanks were inserted into and retrieved from cortical tissue without buckling or mechanical damage, confirming that the PSi shank is stiff enough to penetrate into cortical tissue.

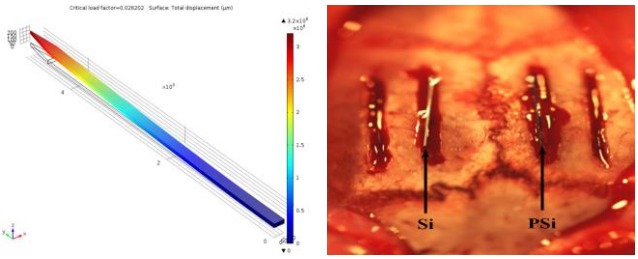

Figure 4: (a) Buckling force simulation for PSi shanks; (b) in vivo insertion test for Si and PSi shanks.

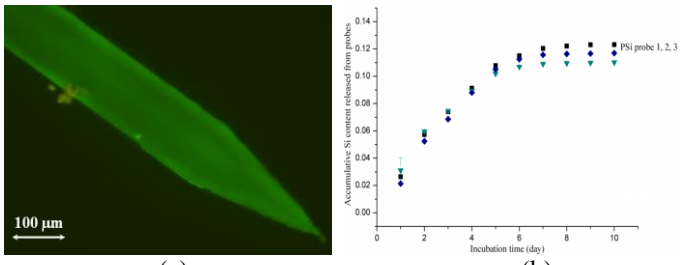

Figure 5: (a) *the PSi shank loading Dex fluorescein; (b) in vitro degradation profile of PSi shanks.*

Due to no space to store Dex fluorescein and rinse by ACSF and DIW, nothing was visualized under the fluorescence microscope for Si shanks. On the contrary, PSi shanks were stained in green under the fluorescence microscopy for the reason that Dex fluorescein solution flowed into the porous structure and the drugs absorbed onto the inner surface of pores once the solution was evaporated (Fig. 5a). Therefore, anti-inflammation drugs/biomoleculars can be loaded into the PSi shank to reduce the acute tissue responses.

Fig. 5b displays the cumulative degradation curves of PSi shanks in ACSF for 10 days. After 7 days of incubation *in vitro*, the PSi shanks almost fully degraded in ACSF, which was nearly consistent with the *in vivo* results (Figure is not shown here, PSi shanks disappeared in rat brain after 7 days of implantation).

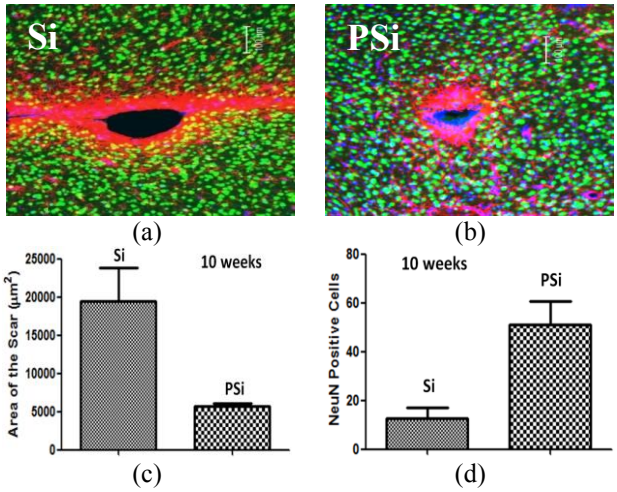

Figure 6:Immunostaining for insertion sit : (a) Si shank and (b) PSi shank (green: neurons, red: astrocytes, blue: cell nuclei); (c) scar area caused by Si and PSi shanks; (d) number of neurons surrounding Si and PSi shanks after 10-week insertion (radium = 160 μm).

After 10 weeks of implantation, immunohistochemical staining of rat brain slices is shown in Fig. 6. Cell nucleuses were stained in blue, while red and green stains represented astrocytes and neurons, respectively (Fig. 6a and b). The scar area caused by PSi shanks was less than one third of that of Si shanks (Fig. 6c), while the number of neurons surrounding PSi shanks was 3 times higher in comparison with Si shanks, in the area with the radium of 160 um at insertion sites (radium = 160 μm, Fig. 6d). Therefore, host tissue responses were suppressed due to the degradation of PSi shanks and subsequent reduced stiffness mismatch between implant and cortical tissue.

CONCLUSIONS

A CMOS compatible microfabrication process was proposed to successfully develop a mechanically adaptive PSi-parylene neural probe. As a mechanical element to strength the neural probe and facilitate probe insertion, PSi shank not only has capability to load anti-inflammation drugs/biomoleculars to attenuate the acute tissue responses, but also dissolves *in vitro* and *in vivo* to leave only the flexible parylene structure. As a consequence of PSi shank degradation and minimized stiffness mismatch between implant and cortical tissue, host tissue responses (e.g. glial scar area surrounding the neural probe) were significantly reduced. Therefore, the novel strategy for reliable BMI is expected to remarkably enhance the long-term recording stability of neural probes.

ACKNOWLEDGEMENTS

This work was supported by the Science andEngineering Research Council of Agency for Science, Technologyand Research (A*STAR) under Grant 1021710159.

REFERENCES

[1] S. Senturia, “Perspectives on MEMS Past and Future: the Tortuous Pathway from Bright Ideas to Real Products”, in *Digest Tech. Papers Transducers‘03 Conference*, Boston, June 8-12, 2003, pp. 10-15.

[2] T. Tsuchiya, O. Tabata, J. Sakata, Y. Taga, “Specimen Size Effect on Tensile Strength of Surface Micromachined Polycrystalline Silicon Thin Films”, *J. Microelectromech. Syst.*, vol. 7, pp. 106-113, 1998.

[3] R. P. Feynman, *Lectures on Physics*, Addison Wesley, 1989.

[1] V.S. Polikov, P.A. Tresco, W.M. Reichert, “Response of brain tissue to chronically implanted neural electrodes”, *J. Neurosci.Methods*, vol. 148, pp. 1-18, 2005.

[2] P. Fattahi, G. Yang, G. Kim, M.R. Abidian, “A Review of Organic and Inorganic Biomaterials for Neural Interfaces”, *Adv. Mater.*, vol. 26, pp. 1846-1885, 2014

[3] J.P. Seymour, D.R. Kipke, “Neural Probe Design for Reduced Tissue Encapsulation in CNS”, *Biomaterials*, vol. 28, pp. 3594-3607, 2007.

[4] B.J. Kim, B. Chen, M. Gupta, E. Meng, “Formation of Three-Dimensional Parylene C Structures via Thermoforming”, *J. Micromech. Microeng.,* vol. 24, pp. 065003, 2014.

[5] M.R. Abidian, D.C. Martin, “Multifunctional Nanobiomaterials for Neural Interfaces”, *Adv. Funct. Mater.,* vol. 19, pp. 573-585, 2009.

[6] F. Wu, L.W. Tien, F. Chen, J.D. Berke, D.L. Kaplan, E. Yoon, “Silk-backed Structural Optimization of High-density Flexible Intracortical Neural Probes”, *J. Microelectromech. Syst.*, vol. 24, pp. 62-69, 2015.

[7] W.M. Tsang, A.L. Stone, D. Otten, Z.N Aldworth, T.L. Daniel, J.G. Hildebrand, R.B. Levine, J. Voldman, “ Insect-machine Interface: A Carbon Nanotube-enhanced Flexible Neural Probe”, *J. Neuronsci. Methods* Vol. 204, pp. 355-365, 2012.

[8] T. Sun, W.M. Tsang, W.-T. Park, “Drug Release from Porous Silicon for Stable Neural Interface”, *Appl. Surf. Sci.*, vol. 292, pp. 843-851, 2014.

[9] E.J. Anglin, L. Cheng, W.R. Freeman, M.J. Sailor, “Porous Silicon in Drug Delivery Devices and Materials”, *Adv. Drug Deliv. Rev.*, vol. 60, pp. 1266-1277, 2008.

[10] A.A. Sharp, A.M. Ortega, D. Restrepo, D. Curran-Everett, K. Gall, “In Vivo Penetration Mechanics and Mechanical Properties of Mouse Brain Tissue at Micrometer Scales”, *IEEE Trans. Biomed.Eng.*, vol. 56, pp. 45-53, 2009.

CONTACT

*W.M. Tsang, tel: +852-3406 2611; wmtsang@alumni.cuhk.net
*Y. Gu, tel: +65-67705915; guyd@ime.a-star.edu.sg